Evidence of Inward Toroidal Momentum Convection in the JET Tokamak

T. Tala,[1] K.-D. Zastrow,[2] J. Ferreira,[3] P. Mantica,[4] V. Naulin,[5] A. G. Peeters,[6] G. Tardini,[7] M. Brix,[2] G. Corrigan,[2] C. Giroud,[2] and D. Strintzi[8]

[1]*Association EURATOM-Tekes, VTT, P.O. Box 1000, FIN-02044 VTT, Finland*
[2]*EURATOM/UKAEA Fusion Association, Culham Science Centre, Oxon, OX14 3DB, United Kingdom*
[3]*Associação EURATOM/IST, Instituto de Plasmas e Fusão Nuclear, 1049-001 Lisbon, Portugal*
[4]*Istituto di Fisica del Plasma CNR-EURATOM, via Cozzi 53, 20125 Milano, Italy*
[5]*Association Euratom-Risø DTU, DK-4000 Roskilde, Denmark*
[6]*Center for Fusion, Space and Astrophysics, Department of Physics, University of Warwick, CV4 7AL, United Kingdom*
[7]*Max-Planck-Institut für Plasmaphysik, EURATOM-Assoziation, D-85748, Garching, Germany*
[8]*National Technical University of Athens, Euratom Association, GR-15773 Athens, Greece*

(Received 22 May 2008; published 17 February 2009)

Experiments have been carried out on the Joint European Torus tokamak to determine the diffusive and convective momentum transport. Torque, injected by neutral beams, was modulated to create a periodic perturbation in the toroidal rotation velocity. Novel transport analysis shows the magnitude and profile shape of the momentum diffusivity are similar to those of the ion heat diffusivity. A significant inward momentum pinch, up to 20 m/s, has been found. Both results are consistent with gyrokinetic simulations. This evidence is complemented in plasmas with internal transport barriers.

DOI: 10.1103/PhysRevLett.102.075001 PACS numbers: 52.25.Fi, 52.35.Ra, 52.55.Fa

Plasma rotation and momentum transport in tokamaks are currently a very active research area. Sheared rotation can lead to quenching of turbulence and a subsequent improvement in confinement [1]. Toroidal rotation also increases stability against pressure limiting resistive wall modes [2]. Still, transport of toroidal momentum is less understood than heat or particle transport. Extrapolating reliably toroidal rotation, in magnitude and profile shape to future tokamaks, such as ITER, remains a challenge, as neither momentum transport nor sources are known precisely.

It is useful to compare momentum and ion heat transport under the conditions where the ion temperature gradient (ITG) instability is dominant, as both transport channels are predicted to be similar [3,4]. The momentum diffusivity χ_ϕ and pinch velocity v_{pinch} (negative sign denotes inwards) are related to the toroidal velocity v_ϕ, its gradient $\nabla_{v\phi}$, and the momentum flux Γ_ϕ, assuming the absence of a significant particle flux, as follows:

$$\Gamma_\phi \sim -\chi_\phi \nabla(v_\phi n) + v_{\text{pinch}} v_\phi n = -\chi_{\phi,\text{eff}} \nabla(v_\phi n), \quad (1)$$

where n is the ion density. It is always possible to combine the diffusive and convective parts of the momentum flux into an effective momentum diffusivity $\chi_{\phi,\text{eff}}$. This quantity can be easily determined from steady-state transport analysis once the sources are known, while the determination of χ_ϕ and v_{pinch} separately requires more sophisticated experiments.

A rotation database covering more than 600 Joint European Torus (JET) discharges shows that the effective Prandtl number $\text{Pr}_{\text{eff}} = \chi_{\phi,\text{eff}}/\chi_{i,\text{eff}} \approx 0.1$–$0.4$ is substantially below one in the JET core plasma [5,6]. The low Pr_{eff} is in apparent contradiction with ITG-based theories and gyrokinetic calculations, which report "purely diffusive" Prandtl number $\text{Pr} = \chi_\phi/\chi_i \approx 1$ [4,7]. Recent developments in theory predict a sizable inward momentum pinch [8,9], possibly resolving the discrepancy of Pr_{eff} being smaller than Pr. Until now, experimental evidence for an inward momentum pinch has been reported on the JT-60U tokamak [10] and National Spherical Torus Experiment tokamak [11]. In this Letter, we present experimental evidence of a significant inward momentum pinch in JET, using torque modulation techniques. This evidence is complemented with observations in plasmas with internal transport barriers (ITBs) showing different dynamic behavior between ion temperature and toroidal velocity.

Studying heat transport by modulation of localized, electron, or ion cyclotron resonance heating is a well-established technique [12]. For momentum, torque from the neutral beam injection (NBI) system can be modulated. Passing ions transfer toroidal angular momentum to the bulk plasma by collisions, which is a slow process, whereas trapped ions transfer their momentum by $\mathbf{j} \times \mathbf{B}$ forces, which is practically instantaneous ($\mathbf{j}$ denotes displacement current density due to finite banana orbit width and $\mathbf{B}$ magnetic field) [13].

An experiment where the NBI power and torque were modulated at 6.25 Hz (NBI 80 ms on and 80 ms off) has been performed on JET. This modulation frequency is much lower than the 10 ms time resolution of the charge exchange recombination spectroscopy diagnostics used to measure the angular toroidal rotation ω_ϕ and ion temperature T_i at 12 radial points [14]. The modulation took place between $t = 4$ s and $t = 13$ s with the total NBI power modulating between 10 and 15 MW. The most interesting time traces are shown in Fig. 1.

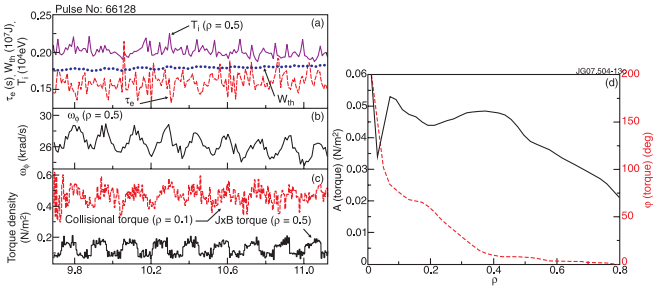

FIG. 1 (color online). Time traces of (a) T_i, stored thermal energy W_{th}, and confinement time τ_E, (b) toroidal angular frequency ω_ϕ, (c) two components of the torque density for JET pulse 66 128. (d) Amplitude (solid black line) and phase (dashed red line) of the modulated total torque.

To perform the cleanest possible ω_ϕ modulation and to avoid MHD modes, an H-mode plasma with type III edge localized modes, low collisionality, and high q_{95} was chosen. Under these conditions, ITG is the dominant instability, making the coupling of momentum and ion heat transport, and thus the concept of the Prandtl number, unambiguous.

The NBI-induced torque has been calculated with the NUBEAM code [15] inside the TRANSP transport code. No Alfvén eigenmode activity or any other MHD mode, such as sawtooth, is observed that could redistribute NBI-driven fast ions and further have an impact on the calculated torque profiles from TRANSP. To obtain a torque modulation signal far beyond noise, 160 000 particles have been used in the Monte Carlo calculation of NBI torque. All phases are calculated with reference to the phase of the NBI power. The calculated amplitude and phase at 6.25 Hz of the modulated torque density profiles are shown in Fig. 1(d) as a function of the normalized toroidal flux coordinate. Outside $\rho > 0.4$, the torque is dominated by the $\mathbf{j} \times \mathbf{B}$ component and synchronous with the injected power, while in the central part of the plasma, the collisional component dominates, resulting in a delay of about 50 ms due to the slowing down time of the fast ionized beam particles. Very similar torque density profiles as those from TRANSP have been calculated with the ASCOT orbit-following Monte Carlo code [16]. The intrinsic rotation is not expected to be modulated either as the modulation in W_{th} is only about 1% [shown in Fig. 1(a)] resulting from the modulation in temperatures of similar order 1%–2% (no modulation in n_e). Furthermore, other torque sources or sinks, such as a torque due to fast ion losses originating from toroidal magnetic field ripple, ion cyclotron resonance heating-driven rotation, or plasma braking due to intrinsic error fields in these low β plasmas, are negligible as compared with the NBI-driven torque. As the modulated torque is not radially localized, a simple determination of χ_ϕ and v_{pinch} directly from the spatial derivatives of the amplitude and phase of the modulated ω_ϕ is not viable. Therefore, time-dependent transport modeling of ω_ϕ is required.

The novel methodology in this study to determine χ_ϕ and v_{pinch} uses the following 3 steps: step 1, calculate $\chi_{i,\text{eff}}$; step 2, vary the Pr value and its radial profile to fit the simulated phase of modulated ω_ϕ to the experimental phase profile, as χ_ϕ is the main contributor to the phase while v_{pinch} plays only a minor role, as shown in Ref. [17]; step 3, vary v_{pinch} to best fit also the simulated amplitude of the modulated ω_ϕ to the experimental data, simultaneously also matching the steady state. In step 1, $\chi_{i,\text{eff}}$ is calculated from the measured T_i data and calculated power deposition profiles. No ion heat pinch is assumed, a result supported in recent T_i modulation experiments [18]. Step 2 leads to a rather precise identification for the range of Pr values, since Pr is the only unknown. This resolves the indeterminacy associated with the analysis of only the steady-state profile, as the latter can be reproduced by an unlimited number of possible combinations for χ_ϕ and v_{pinch} yielding the same $\chi_{\phi,\text{eff}}$. Once Pr is identified, step 3 allows us to identify v_{pinch} needed to reproduce the steady state ω_ϕ and amplitude with the chosen Pr value.

Figures 2 and 3 compare experimental data and simulations for the ω_ϕ steady state and modulated amplitude $A_{\omega,\phi}$ and phase $\phi_{\omega,\phi}$. The experimental profiles have been mapped onto a moving equilibrium to eliminate the spurious modulation components due to modulated plasma position. For the simulations, the two most obvious options for χ_ϕ or Pr and v_{pinch} were adopted: (i) Fix Pr = 0.25 to yield $\chi_\phi = 0.25\chi_{i,\text{eff}}$ and $v_{\text{pinch}} = 0$, or (ii) match the simulated and experimental phase by fitting Pr, using the profile shape from gyrokinetic simulations with the gyrokinetic Warwick (GKW) code [19] and then vary the v_{pinch} profile to additionally match the simulated and experimental amplitudes and steady state. All simulations have been performed with the JETTO transport code. The transport equation for ω_ϕ is solved while q, T_i, T_e, and n_e are frozen to their experimental values. The boundary conditions for steady state ω_ϕ and the amplitudes $A_{\omega,\phi}$ and phases $\phi_{\omega,\phi}$ of the modulated ω_ϕ are chosen to fit the experimental data

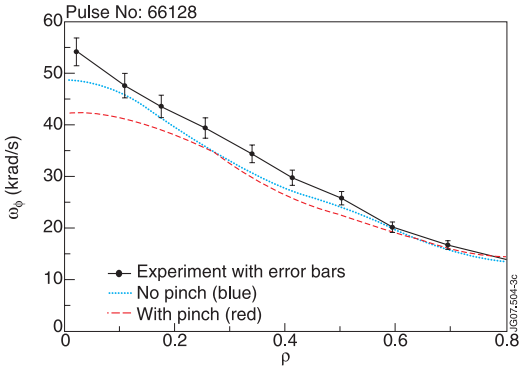

FIG. 2 (color online). The simulated steady state ω_ϕ with the two options (i) (dotted blue line) and (ii) (dashed red line) compared with the experimental ω_ϕ (solid black line) with error bars.

at $\rho = 0.8$. The transport simulations are carried out over the 9 modulation cycles shown in Fig. 1.

Both simulations (i) and (ii) predict the steady state ω_ϕ within 10% accuracy in the region of interest, i.e., $0.2 < \rho < 0.8$, as seen in Fig. 2. Inside $\rho < 0.2$, neoclassical transport starts to dominate ion heat transport, and the predictions are worse as the use of the ITG-based Pr for calculating χ_ϕ is not appropriate.

Options (i) and (ii) differ, however, in reproducing the $A_{\omega,\phi}$ and $\phi_{\omega,\phi}$ profiles as shown in Fig. 3. Case (i) with $P_r = 0.25$ and $v_{\text{pinch}} = 0$ clearly disagrees with the experiments. The simulated phase is too large, an indication of too low χ_ϕ (too low Pr) used in the simulation. On the other hand, the simulated amplitude is too low towards the plasma center, which could be cured only by lowering χ_ϕ further. This shows that the assumption $v_{\text{pinch}} = 0$ is not compatible with the experiments. Case (ii) uses $\text{Pr} = \chi_\phi/\chi_i \sim 1$ [Fig. 3(c)] and v_{pinch} varying radially between 0 and -25 m/s [Fig. 3(d)]. This improves the agreement between the simulated and experimental amplitudes and phases dramatically. This v_{pinch} profile reproduces best the experimental $A_{\omega,\phi}$ and $\phi_{\omega,\phi}$ profiles and the steady state ω_ϕ. Uniform $\text{Pr} = 1.0$ instead of using Pr profile from the GKW model with the same v_{pinch} results in almost as good agreement with experiment. Finally, while the Pr numbers from the GKW model are in excellent agreement with experiment, there is some discrepancy in the pinch numbers, defined as $Rv_{\text{pinch}}/\chi_\phi$. The pinch numbers from the GKW model are 2–4, depending on radius, whereas the experimental ones are in the range of 3–8.

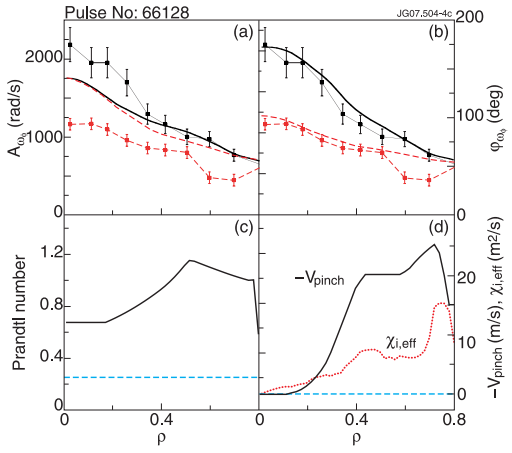

FIG. 3 (color online). Comparison of the experimental amplitude (black solid line with error bars) and phase (red dashed line with error bars) and simulated amplitudes $A_{\omega,\phi}$ (black solid line) and phases $\phi_{\omega,\phi}$ (red dashed line) of modulated $\omega\varphi$ in (a) case (i) with $\text{Pr} = 0.25$ and $v_{\text{pinch}} = 0$ and (b) case (ii) with $\text{Pr} \approx 1$ and v_{pinch} taken from (d) (black solid line). (c) Prandtl numbers and (d) pinch velocity profiles used in cases (i) (blue dashed line) and (ii) (black solid line). Also shown the used $\chi_{i,\text{eff}}$ (red dotted line) in (d).

A sensitivity analysis shows that 20%–30% variability in Pr and v_{pinch} is compatible with experimental data, while outside this range the simulated phase and amplitude deviate unacceptably from the experimental values. The TRANSP torque calculations have been found very robust with respect to variations in plasma parameters.

One complicating factor requiring a careful assessment is that T_i and T_e are also modulated with peak amplitudes around 70 eV, i.e., a perturbation of about 1% to be compared with the amplitude of the ω_ϕ modulation being around 4%. A time variation of T_i and its gradient length induces a time variation in the ITG-driven transport, causing an oscillation in χ_i. This leads to an oscillation in χ_ϕ, yielding an extra contribution to $A_{\omega,\phi}$ and $\varphi_{\omega,\phi}$ and possibly modifying the determined Pr and v_{pinch}. To estimate the impact of such T_i modulation on the determined Pr and v_{pinch}, a time-dependent χ_i using an ion heat transport model based on the critical gradient length concept [20] and with typical parameters found in JET ion heat transport studies [18] has been used to model the modulated T_i and the associated time variation of χ_i and χ_ϕ. Owing to the small amplitude of the T_i modulation (the amplitude of χ_i is 1%–2% depending on the radius), the effect on the values determined for Pr and v_{pinch} was insignificant. The insensitivity of Pr and v_{pinch} to the temperature modulation and to the variations in the input profiles together with mapping the profiles onto a plasma movement independent coordinate have resulted in robust estimates for the profiles and magnitudes of Pr and v_{pinch}, as compared with the preliminary analysis shown in Ref. [6].

Additional evidence of the existence of inward momentum pinch on JET comes from a plasma with an ITB. It has been reported that the foot point of the ITB coincides among all transport channels (T_i, T_e, n_e, ω_ϕ) [21]. The present experimental observation, however, illustrates that the foot point of the ITB seems to be located at a slightly larger radius in T_i than in ω_ϕ as the ITB moves radially outwards. In Fig. 4, the T_i barrier is located within the charge exchange recombination spectroscopy (CXRS) channel [marked as horizontal lines in Fig. 4(d)] centered at $r/a = 0.48$, whereas the ω_ϕ barrier is located one CXRS channel more inwards, i.e., centered at $r/a = 0.41$ at $t = 5.29$–5.31 s. This can be seen clearly in Figs. 4(c) and 4(d), where there is virtually no difference in $\Delta\omega_\phi$ while there is a significant difference in ΔT_i at $r/a = 0.48$. At $t = 5.35$ s, the ω_ϕ barrier also appears at $r/a = 0.48$. The ITB moves steadily outwards, following the outward movement of the $q_{\min}$ surface, the foot point reaching a radius $r/a = 0.65$ until the ITB collapses at $t = 5.95$ s. During its radial outward movement, the ITB passes two other CXRS channels at $r/a = 0.58$ at $t = 5.34$ s and $r/a = 0.66$ at $t = 5.77$ s. Both times, the ITB is seen first in T_i and after a few tens of milliseconds in ω_ϕ, indicating that the foot point of the ITB is indeed located at a more outward radius for T_i than for ω_ϕ.

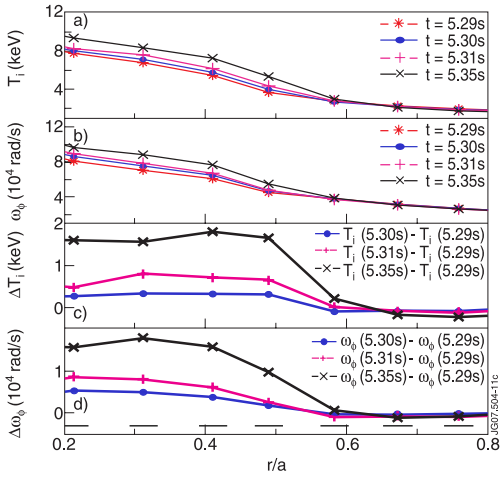

FIG. 4 (color online). (a) T_i, (b) ω_ϕ, (c) ΔT_i, and (d) $\Delta\omega_\phi$ profiles for JET pulse 69 670 during the radial expansion of the ITB. The horizontal lines shown in (d) indicate the radial widths of the CXRS measurements points.

To understand this, two hypotheses have been tested: (i) In the absence of v_{pinch}, ω_ϕ could respond more slowly than T_i to the turbulence suppression within the ITB as $\chi_{i,\text{eff}}$ is larger than $\chi_{\phi,\text{eff}}$, and (ii) an inward toroidal momentum pinch causes an apparent delay to the outward movement of the ITB in the ω_ϕ channel. Predictive transport simulations for T_i and ω_ϕ have been performed, with initial conditions for T_i and ω_ϕ taken from pulse 69 670. The ITB in T_i is simulated by moving the low χ_i region outwards with time. For momentum transport, the two options (i) and (ii) are applied. In the simulation with $\text{Pr}_{\text{eff}} = 0.3$ and $v_{\text{pinch}} = 0$, T_i and ω_ϕ react to the change of χ_i in the same way, resulting in the foot point of the ITB being exactly the same. In case (ii), the v_{pinch} profile is assumed to be proportional to χ_i and normalized to the value consistent with the value found in the NBI modulation experiment ($v_{\text{pinch}} \approx -15$ m/s outside the ITB). This simulation shows that ω_ϕ responds more slowly to the radial outward movement of the ITB than T_i at the location of the ITB, as seen in Fig. 5. This is consistent with the CXRS measurements showing the rise of T_i just before the rise of ω_ϕ when the ITB passes the CXRS channel during its radial outward movement.

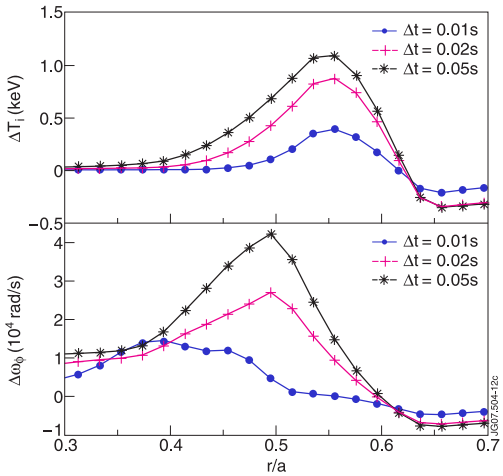

FIG. 5 (color online). As in Fig. 4, but for simulated (a) ΔT_i and (b) $\Delta\omega_\phi$ profiles with a model of $v_{\text{pinch}} \approx -15$ m/s and $\text{Pr} = 1.0$.

In summary, consistent evidence for a significant inward momentum pinch has been found in JET. This may have important implications on the predictions for the toroidal velocity profile in ITER. In particular, a centrally peaked toroidal velocity profile might still result even in the absence of any external core momentum source. It still remains to be assessed if the parametric dependencies of such a pinch term are such that a convective component could possibly be present in ITER.

This work, supported by the European Communities under the contract of Association between EURATOM and Tekes, was carried out within the framework of the European Fusion Development. This work was done under the JET-EFDA workprogram [22].

[1] H. Biglari *et al.*, Phys. Fluids B **2**, 1 (1990).
[2] A. M. Garofalo *et al.*, Nucl. Fusion **41**, 1171 (2001).
[3] N. Mattor *et al.*, Phys. Fluids **31**, 1180 (1988).
[4] A. G. Peeters *et al.*, Phys. Plasmas **12**, 072515 (2005).
[5] P. C. de Vries *et al.*, Plasma Phys. Controlled Fusion **48**, 1693 (2006).
[6] T. Tala *et al.*, Plasma Phys. Controlled Fusion **49**, B291 (2007).
[7] D. Strintzi *et al.*, Phys. Plasmas **15**, 044502 (2008).
[8] A. G. Peeters *et al.*, Phys. Rev. Lett. **98**, 265003 (2007).
[9] T. S. Hahm *et al.*, Phys. Plasmas **14**, 072302 (2007).
[10] M. Yoshida *et al.*, Nucl. Fusion **47**, 856 (2007).
[11] W. Solomon *et al.*, Phys. Rev. Lett. **101**, 065004 (2008).
[12] N. J. Lopez Carzodo, Plasma Phys. Controlled Fusion **37**, 799 (1995).
[13] K.-D. Zastrow *et al.*, Nucl. Fusion **38**, 257 (1998).
[14] C. R. Negus *et al.*, Rev. Sci. Instrum. **77**, 10F102 (2006).
[15] A. Pankin *et al.*, Comput. Phys. Commun. **159**, 157 (2004).
[16] J. A. Heikkinen *et al.*, J. Comput. Phys. **173**, 527 (2001).
[17] P. Mantica *et al.*, Nucl. Fusion **32**, 2203 (1992).
[18] F. Ryter *et al.*, in *Proceedings of the 22nd International Conference on Fusion Energy, Geneva, 2008* [International Atomic Energy Agency (IAEA), Vienna, 2008], paper EX/P5-19.
[19] A. G. Peeters *et al.*, Phys. Plasmas **11**, 3748 (2004).
[20] X. Garbet *et al.*, Plasma Phys. Controlled Fusion **46**, 1351 (2004).
[21] C. D. Challis *et al.*, Plasma Phys. Controlled Fusion **44**, 1031 (2002).
[22] F. R. Romanelli *et al.*, in *Proceedings of the 22nd International Conference on Fusion Energy, Geneva, 2008* [International Atomic Energy Agency (IAEA), Vienna, 2008]. (All of the members of the JET-EFDA Collaboration appear in the appendix of this paper.)